

## Confinement Effects at the External Surface of Delaminated Zeolites (ITQ-2): An Inorganic Mimic of Cyclodextrins

María S. Galletero, Avelino Corma,\* Belén Ferrer, Vicente Fornés, and Hermenegildo García\*

Instituto de Tecnología Química CSIC UPV, Universidad Politécnica de Valencia,  
Avda de los Naranjos s/n, 46022-Valencia, Spain

Received: April 25, 2002; In Final Form: September 5, 2002

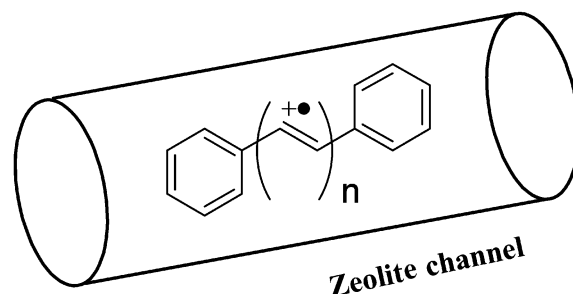
Novel delaminated ITQ-2 zeolite has a remarkably large accessible external surface area ( $\sim 800 \text{ m}^2 \text{ g}^{-1}$ ) and reduced microporosity ( $0.009 \text{ cm}^{-3} \text{ g}^{-1}$ ) and has attracted interest as an alternative to conventional zeolites or mesoporous MCM-41 (Corma, A.; Fornés, V.; Pergher, S. B.; Maesen, T. L. M.; Buglass, J. G. *Nature* **1998**, 396, 353–356).  $\alpha,\omega$ -Diphenyl polyenes have been used as molecular probes to check the ability of ITQ-2 zeolite to generate organic radical cations. Of these probes, only *t,t*-1,4-diphenyl-1,3-butadiene (DPB) is transformed into a persistent reaction intermediate upon adsorption on ITQ-2. The process occurs in the “cup”-like cavities open to the exterior since selective silylation of the cups inhibits completely the generation of this reaction intermediate. Detection of 1-phenylnaphthalene as reaction product, EPR spectroscopy, and alternative laser flash photolysis generation strongly support 1-phenylnaphthalene radical cation as the intermediate formed after the adsorption of DPB onto ITQ-2. This contrasts with the behavior of conventional zeolites ZSM-5 and mordenite in which  $\text{DPB}^{+\cdot}$  is the only species formed and demonstrates the uniqueness of the behavior of ITQ-2 as result of its unprecedented topology.

### Introduction

$\alpha,\omega$ -Diphenyl polyenes have been used as probe molecules to demonstrate the ability of zeolites to generate a high population of persistent organic radical cations.<sup>1,2</sup> These molecules present the advantage of having similar kinetic diameter and molecular shape, varying exclusively the chain length and the oxidation potential, which gradually decreases as the number of C=C increases. It was found that these  $\alpha,\omega$ -diphenyl polyenes may form indefinitely persistent radical cations when they are incorporated within the channels of medium pore size ZSM-5 zeolite.<sup>3,4</sup> It was proposed that the terminal phenyl rings, tightly fitting with the zeolite framework, protect the inner polyene bridge bearing the unpaired electron (Scheme 1). The role of phenyl rings acting as stoppers in the channels of ZSM-5, as originally proposed, was also expanded to other types of organic reactive intermediates such as  $\alpha,\omega$ -diphenyl allyl cations.<sup>5</sup> In addition to ZSM-5, the fate of  $\alpha,\omega$ -diphenyl polyenes on other conventional zeolites such as Y, Beta, and mordenite has also been studied in an attempt to establish a relationship between the zeolite structure and the ability to generate persistent organic radical cations.<sup>1,3,4,6</sup>

In recent years, many novel zeolite structures have been synthesized. It is therefore of interest to study the behavior of well-documented probes with novel zeolitic materials in order to assess whether new topological effects, not previously found in conventional zeolites, can be observed. In fact, given the importance of zeolites from an economical point of view, the synthesis of novel structured porous materials constitutes a very active area of research.<sup>7–10</sup> In this regard, the preparation of mesoporous aluminosilicates of the MCM-41 type was a significant breakthrough because these materials combine a very large surface area and a regular pore size, the latter being controlled during the synthesis (20–100 nm).<sup>11</sup> The ability of mesoporous MCM-41<sup>12,13</sup> to generate a stationary population

### SCHEME 1



of organic radical cations is generally very low, something that agrees with the previous tight-fit paradigm to rationalize the persistence of radical cations. Given the large dimensions of the channels of MCM-41, most organic radical cations will experience a loose fit and will not be protected from nucleophilic attacks.

In this context, a new type of zeolitic material described as delaminated zeolites has been recently reported.<sup>14</sup> One example of such materials is the zeolite ITQ-2 that was prepared from the layered precursor of MCM-22 by delamination of the swollen precursor followed by calcination (Scheme 2). The ITQ-2 solid is formed by an array of disordered zeolitic layers. These layers are essentially those found in the MCM-22 precursor and they encompass two different topological units consisting of open cups of  $\sim 7 \text{ \AA}$  of diameter and  $\sim 8 \text{ \AA}$  depth located at the upper and lower planes of the layers and independent, not connected, sinusoidal 10-membered ring (10 MR) intralayer channels. Figure 1 shows the structure of the ITQ-2 layers wherein these two morphological components have been highlighted.

Given that the topology and geometrical features of ITQ-2 are not encountered in any conventional zeolite, it is of interest to address whether the very large external surface ( $\sim 800 \text{ m}^2 \text{ g}^{-1}$ ) of these materials behaves as a geometrically nonsensitive

\* Corresponding authors.

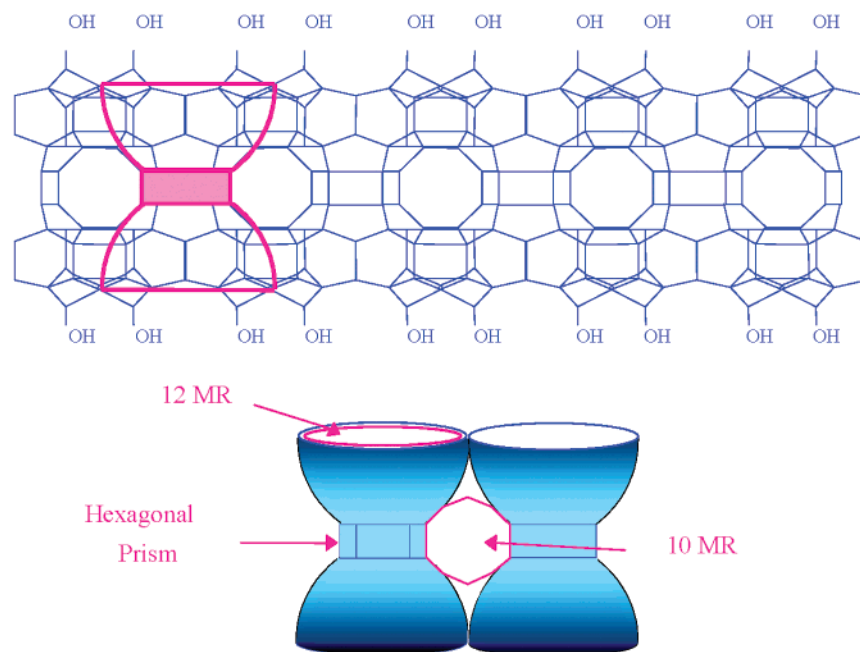
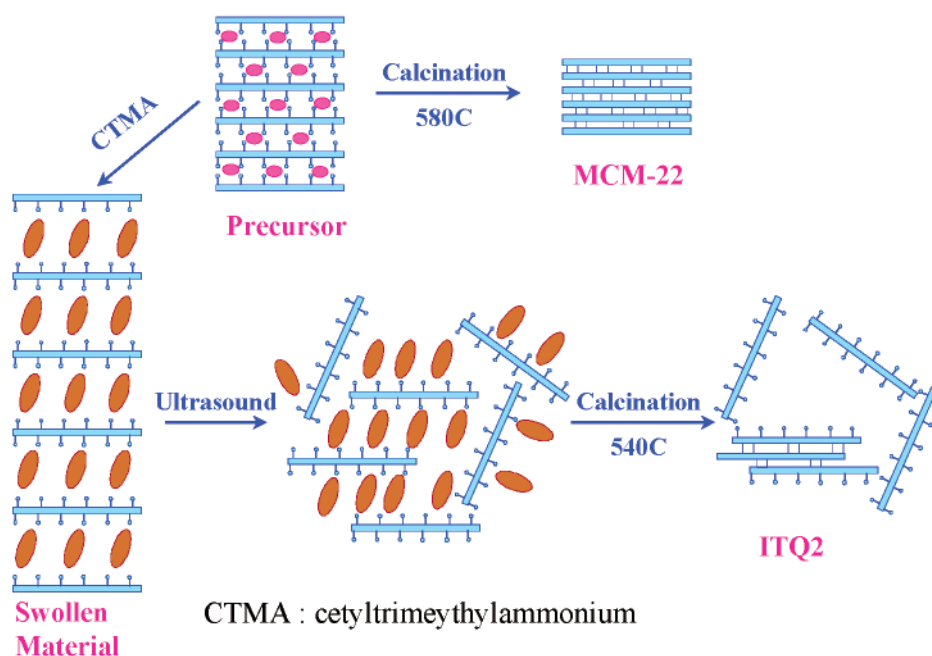


**Figure 1.** Structure of the ITQ-2 layers showing the two morphological components (cups and channels) defined by the framework.

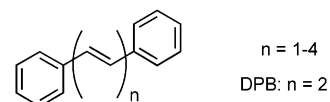
#### SCHEME 2



surface or whether, on the contrary, molecules can experience a well-structured external surface with open cups wherein molecular confinement may occur. If the latter case, it should be possible to generate a significant population of persistent organic radical cations, even though these radical cations would be not located deep inside the zeolite particle but in the shallow layer of the external surface. The aim of this research is to establish whether the structured external surface area of ITQ-2, being easily accessible like that of MCM-41, shares or not with zeolites the characteristic behavior observed in the confined spaces of zeolites.

To address this point we have selected  $\alpha,\omega$ -diphenyl polyenes that constitute a homogeneous series of probes wherein the molecular properties change regularly and for which sufficient information about their behavior in conventional zeolites is

available.<sup>3,4,6</sup> For the present study we have used as probes  $\alpha,\omega$ -diphenyl polyenes from 1 to 4 C=C double bonds.



These molecules are expected to diffuse freely into the open cups of ITQ-2, but on the contrary it is anticipated that diffusion into the 10 MR sinusoidal pores present in the layer of this material should be considerably more impeded due to the continuous direction change of the channels.<sup>15</sup>

#### Experimental Section

$\alpha,\omega$ -Diphenyl polyenes, 1-PNH and TP<sup>+</sup> (as a BF<sub>4</sub><sup>-</sup> salt) were commercial samples and used as received. ZSM-5 and ITQ-2

**TABLE 1: Relevant Physicochemical Parameters of the Porous Aluminosilicates Used in the Present Work**

zeolite	Si/Al ratio	BET surface area (m <sup>2</sup> /g)	crystal size (μm)	external surface area (m <sup>2</sup> /g)	micropore volume (cm <sup>3</sup> /g)	topological characteristics
ZSM-5	≈40	386	0.5–1	46.26	0.111	microporosity internal surface
Na–mordenite	6.5	356	0.1–0.5	20.23	0.165	microporosity internal surface
MCM-22	50	400	≈1	~150	0.121	microporosity internal surface
ITQ-2	58	806	<0.5	750	0.009	no microporosity external surface
Al/MCM-41	13	874	0.1–0.3	~150	0.46	mesoporosity internal surface

were prepared by hydrothermal sol–gel crystallization according to the detailed procedures reported in the literature.<sup>14,32</sup> The crystal structure of the synthesized aluminosilicates was confirmed by powder X-ray diffraction. Silylation of ITQ-2 was carried out by stirring a suspension of the dehydrated layered ITQ-2 zeolite (1 g) with hexamethyldisilazane (0.5 g) in toluene (25 mL) at reflux temperature for 2 h. After this time, the solid was filtered, exhaustively washed with CH<sub>2</sub>Cl<sub>2</sub> and dried. Adsorption of  $\alpha,\omega$ -diphenyl polyenes on the solids was carried out by stirring magnetically, at reflux temperature for 2 h, a suspension of the organic compound (10 mg) in isooctane (5 mL) in the presence of the corresponding solid (180 mg) that had been previously dehydrated by heating at 500 °C overnight. The solid was filtered, washed with fresh solvent (5 mL), dried under vacuum and stored in closed vials at the ambient. 1-PNH was identified by comparison with a commercial sample. Cis isomer of DPN was obtained by 250 W mercury lamp irradiation through Pyrex of a 10<sup>-2</sup> M solution of DPB in hexane for 3 h. Diffuse reflectance UV–Vis spectra were recorded using a Cary 5 spectrophotometer adapted with a “praying mantis” diffuse reflectance accessory and using pristine ZSM-5 as reference. FTIR spectra of pyridine and 2,6-di-*tert*-butylpyridine adsorption on ITQ-2 before and after silylation were recorded in a Nicolet 710 FT spectrophotometer using greaseless quartz cells having CaF<sub>2</sub> windows and a stopcock valve that allowed them to be sealed under high vacuum. Pyridine and 2,6-di-*tert*-butylpyridine vapors were admitted at room temperature at 10<sup>-1</sup> Pa onto dehydrated silylated and unsilylated ITQ-2 samples placed in the IR cell. The cell was evacuated at 250 °C under 10<sup>-2</sup> Pa for 1 h and the intensity of the IR spectra corresponding to the residual retained pyridine compared for the two samples. EPR spectra were recorded at –200 °C on a Bruker ER200D spectrometer working at the X band (9.65 GHz) and using DPPH ( $g = 2.0036$ ) as reference. Laser flash photolysis experiments were carried out using for excitation the third (355 nm,  $\leq 20$  mJ×pulse<sup>-1</sup>) harmonic of a Surelite Nd:YAG laser (pulse  $\leq 10$  ns). The signal from the monochromator/photomultiplier detection system were captured by a Tektronix MDSA digitizer and transferred to computer that controlled the experiment and provides suitable processing and data storage capabilities. Fundamentals and details of similar time-resolved diffuse reflectance laser setup has been published elsewhere.<sup>34</sup>

## Results and Discussion

Compared to conventional zeolites, the delaminated ITQ-2 exhibits a much larger surface area (predominantly external) with a reduced microporosity. In this regard, the ITQ-2 zeolite is similar to MCM-41 in terms of having a large accessible surface, but the zeolite ITQ-2 layers are crystalline and they contain smaller cavities rather than mesoporous channels. Table 1 summarizes the main physicochemical and textural parameters of the samples used in the present work. In this table the major differences of ITQ-2 compared with conventional zeolites and mesoporous MCM-41 have been remarked.

Incorporation of *t*-1,2-diphenylethylene, *t,t*-1,6-diphenyl-1,3,5-hexatriene and *all trans*-1,8-diphenyl-1,3,5,7-octatetraene

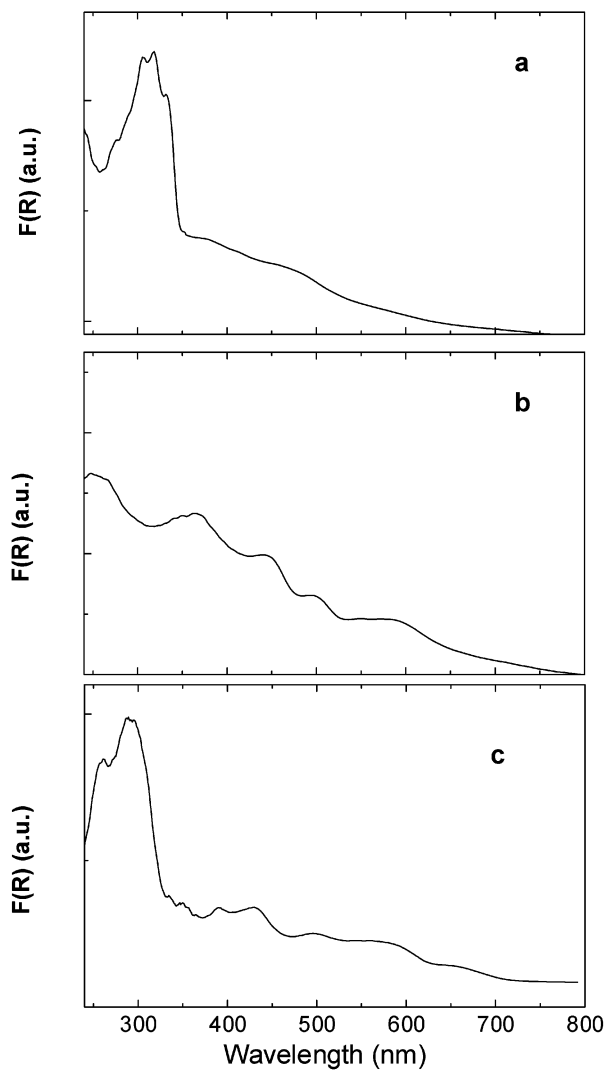


**Figure 2.** Diffuse reflectance UV–vis spectra (plotted as the Kubelka–Munk function  $F(R)$ ) of stilbene (a) *t,t,t*-1,6-diphenyl-1,3,5-hexatriene (b) and *all trans*-1,8-diphenyl-1,3,5,7-octatetraene (c) adsorbed on ITQ-2.

from isooctane solutions onto ITQ-2 does not give the characteristic optical spectra reported for the radical cations of these compounds in ZSM-5 and other zeolites (see Figure 2). We notice that in the case of *t,t,t*-1,6-diphenyl-1,3,5-hexatriene although the diffuse reflectance UV–Vis spectrum rules out the presence of the corresponding radical cation ( $\lambda_{\max}$  597 nm shoulder 540, 766, and 802 nm), some extra bands in addition to those of the starting material can be observed. Something similar happens for *all trans*-1,8-diphenyl-1,3,5,7-octatetraene. On the other hand, we have been able to reproduce the results reported for these three  $\alpha,\omega$ -diphenyl polyenes in conventional acidic ZSM-5 in which the corresponding radical cations are formed.<sup>1</sup>

In sharp contrast, adsorption of *t,t*-1,4-diphenyl-1,3-butadiene (DPB) gives a well defined optical spectrum different totally

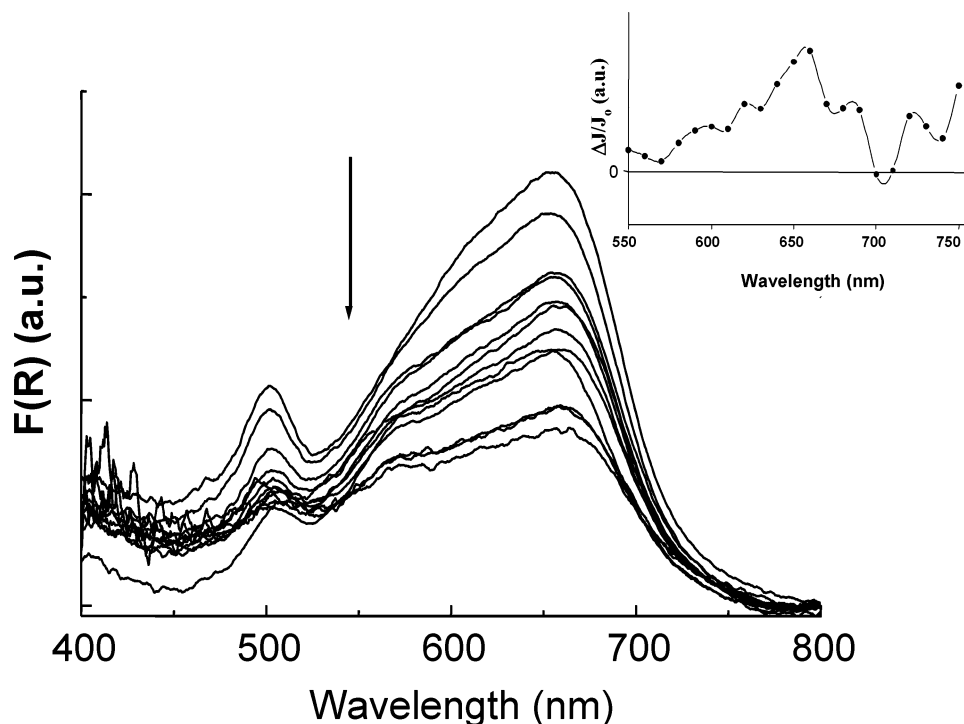


**Figure 3.** Diffuse reflectance UV-vis spectra of DPB@ITQ-2 sample (recorded periodically every week since its preparation). Inset: transient spectrum of 1-PNH (●). The spectrum has been recorded 1  $\mu$ s after the 355 nm laser flash.

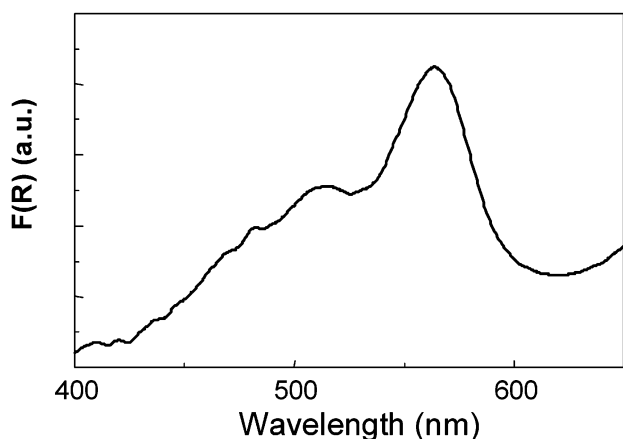


**Figure 4.** Diffuse reflectance UV-vis spectrum (plotted as the Kubelka-Munk function) of DPB@ZSM-5.

from that of the starting material. This spectrum is characterized by a broad absorption band from 550 to 700 nm. The intensity of this absorption band decreases over the time elapsed after sample preparation until a final stationary spectrum is obtained after three months (Figure 3). It is noteworthy that this optical spectrum does not correspond to the DPB<sup>•+</sup> radical cation or to DPBH<sup>+</sup>, the only reaction intermediates previously reported in the incorporation of DPB in acidic zeolites.<sup>1,2</sup> Adsorption of DPB in HY does not give rise to the same transient because the diffuse reflectance spectrum of the DPB@HY is completely different (continuous absorption without resolved peaks). For the sake of comparison, the diffuse reflectance UV-vis spectrum recorded by us for the DPB@ZSM-5 sample under the same conditions, corresponding to DPB<sup>•+</sup> radical cation, is shown in Figure 4.

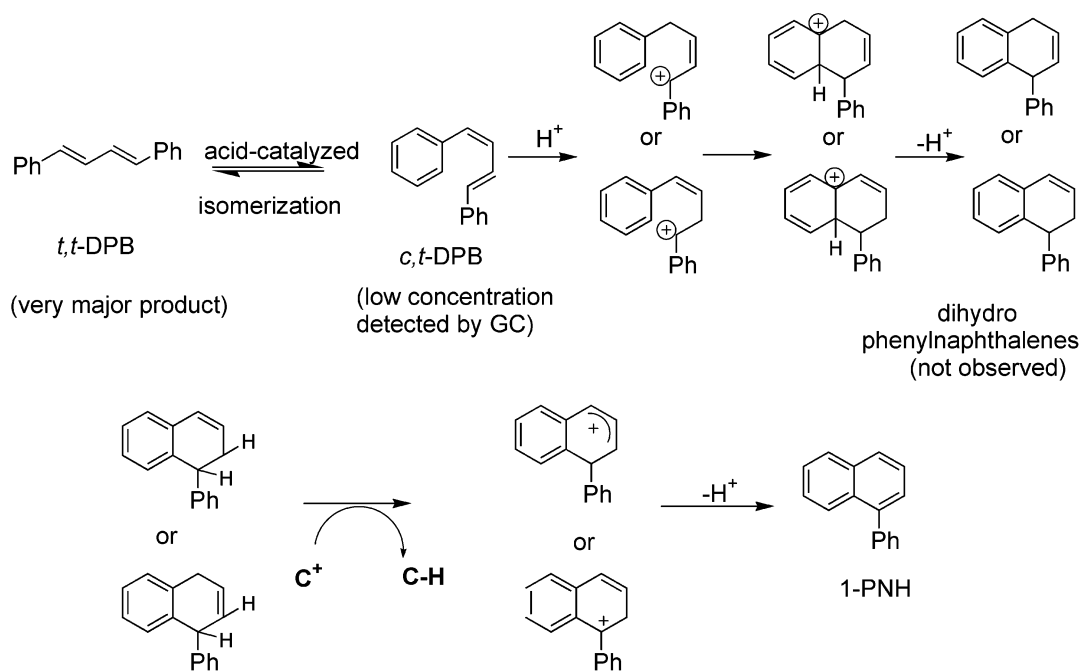
First we have investigated the nature of this unique intermediate responsible for the spectrum shown in Figure 3. When addressing the nature of the adsorbate a good clue is to analyze the reaction mixture after DPB adsorption, looking for products

that could give some hints about the intermediate. In the case here considered, analysis of the solvent after incorporation of DPB and exhaustive solid-liquid extraction of the sample allowed us to observe the presence of 1-phenylnaphthalene (1-PNH) as the only detectable product. In an attempt to confirm that 1-PNH is the immediate precursor of the observed species present in ITQ-2, 1-PNH was adsorbed from a CH<sub>2</sub>Cl<sub>2</sub> onto thermally dehydrated ITQ-2. However, the solid did not become colored and diffuse reflectance UV-vis spectroscopy did not reveal the presence of the 550–700 nm absorption band characteristic of the species generated from DPB. However, when interpreting this negative result it has to be taken into account that the sites/locations accessible for less bulky DPB are not the same as those for 1-PNH which has a larger kinetic diameter and more restricted diffusion.

Two reaction mechanisms (acid catalyzed and electron-transfer mediated) can be envisioned to account the formation of 1-PNH. Thus, to provide evidence about the origin of 1-PNH from DPB, two sets of experiments were carried out in solution. In one of them, an acetonitrile solution of DPB was stirred at room temperature in the presence of catalytic amounts of concentrated sulfuric acid. Under these conditions, cis isomers were formed together with lesser amounts of 1-PNH. This result indicates that DPBH<sup>+</sup> generated from DPB by protonation is able to undergo cyclization to form the dihydronaphthalene skeleton (Scheme 3). It has been reported that adsorption of DPB onto CaY gives 3,4-dihydro-1-phenylnaphthalene together with two other byproducts.<sup>16</sup> Aromatization of this dihydro precursor (compound not observed in the experiments either in ITQ-2 or in sulfuric acid) would be achieved either by oxidation or (most likely in view of the presence of carbocation intermediate) by hydride transfer. Conversion of 3,4-dihydro-1-phenylnaphthalene to 1-PNH through a hydride transfer mechanism has been observed in CaY accompanied with 1-phenyltetraline.<sup>17</sup>

In agreement with these reported results for CaY, our own study adsorbing DPB onto HY in isooctane at 100 °C leads to

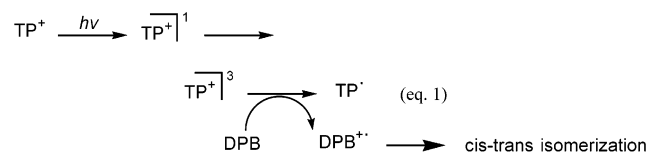
## SCHEME 3



the complete disappearance of the starting material and the formation of one isomer compatible with dihydronaphthalene (60%) together with equal amounts of 1-PNH (21%) and a hydrogenated derivative (19%) tentatively assigned as 1,4-diphenyl-1-butene based on the MS. Minor amounts of a complex mixture of *tert*-butylated products arising from the acid-catalyzed reaction of DPB with isooctane were also observed. This product distribution is also in agreement with Scheme 3 if the hydride acceptor ( $C^+$ ) were  $DPB-H^+$ , whereby 1,4-diphenyl-1-butene could be formed. Interestingly, the HY zeolite did not become colored and, according to the diffuse reflectance UV–vis spectra of the HY zeolite, did not exhibit the 550–700 nm band observed for the case of ITQ-2. Therefore, cyclization of DPB is a general phenomenon that occurs either in solution or in zeolite Y. However, it must be noted that what is unique about cyclodextrin-like ITQ-2 cups is the formation of an unprecedented intermediate as a persistent (month) species.

On the other hand, the possibility that  $DPB^{\bullet+}$  radical cation could also intervene in the formation of 1-PNH was studied by photochemically generating  $DPB^{\bullet+}$  using 2,4,6-triphenylpyrylium cation ( $TP^+$ ) as photosensitizer under aerobic conditions (eq 1).<sup>18</sup>

Laser flash photolysis studies reveal that upon excitation of  $TP^+$  and intersystem crossing to the  $TP^+|^3$  triplet, this excited state is quenched by DPB through an electron transfer mechanism. However, despite the evidences of  $DPB^{\bullet+}$  radical cation generation in the  $TP^+$ -sensitized photolysis, the only photoprocess observed in a preparative irradiation was *cis*–*trans* isomerization, and 1-PNH could not be detected in the reaction mixture. Our observations are consistent with previous reports on the chemical behavior of  $DPB^{\bullet+}$  in which only *cis*–*trans* isomerization was observed<sup>19–27</sup> and rule out the intermediacy of  $DPB^{\bullet+}$  on the formation of 1-PNH.



To further exclude  $DPB^{\bullet+}$  as the reaction intermediate leading to the formation of 1-PNH, laser flash photolysis of DPB adsorbed onto NaY was carried out. NaY being an inert zeolite devoid of acidity does not promote any reaction of DPB. Laser excitation (308 nm) should generate some  $DPB^{\bullet+}$  through photoionization, a general phenomenon known to occur on the polar environment of zeolite pores.<sup>28–30</sup> However, even under these conditions, no evidence for the formation of 1-PNH could be obtained and DPB remained unaltered.

Given that 1-PNH is the only product observed and that the diffuse reflectance UV–vis spectrum of the DPB@ITQ-2 does not probably correspond to any DPB intermediate, we considered the possibility that the spectrum shown in Figure 3 corresponds to a 1-PNH derived intermediate. As a matter of fact, EPR measurements of DPB@ZSM-5 and DPB@ITQ-2 samples (Figure 5) showed a similar spin density. The relative area of the ZSM-5/ITQ-2 EPR signals obtained by double integration was 3.47. Based on previous quantification of the spin count for organic radical cation inside ZSM-5, or estimation that the population of radical cations for the DPB@ZSM-5 and DPB@ITQ-2 is in the order of  $10^{19}$  spin  $\times$  g<sup>-1</sup>, that result corresponds to about 0.5 mg of radical cation per g of zeolite. The comparable amounts of a high population of radical species measured for both samples is compatible with the presence of organic radical ions. Incidentally noteworthy is the fact that the number of spins per gram for ZSM-5 is very similar to ITQ-2, even though the topology of the latter is characterized by the large accessible surface area, compared to the medium pore size channels characteristic of ZSM-5.

The above EPR data suggest that the species present in the DPB@ITQ-2 sample could be the radical cation of 1-PNH. Thus, after formation of 1-PNH from DPB within the ITQ-2 cups, an electron transfer from 1-PNH to the acid sites of the zeolite would generate  $1\text{-PNH}^{\bullet+}$ . Electrochemical measurements in acetonitrile give an oxidation potential for 1-PNH of 1.55 V vs SCE that is comparable to that of the parent naphthalene. The optical spectrum of  $1\text{-PNH}^{\bullet+}$  has not been previously reported. To record the authentic optical spectrum of  $1\text{-PNH}^{\bullet+}$  that could be compared with the diffuse reflectance UV–vis

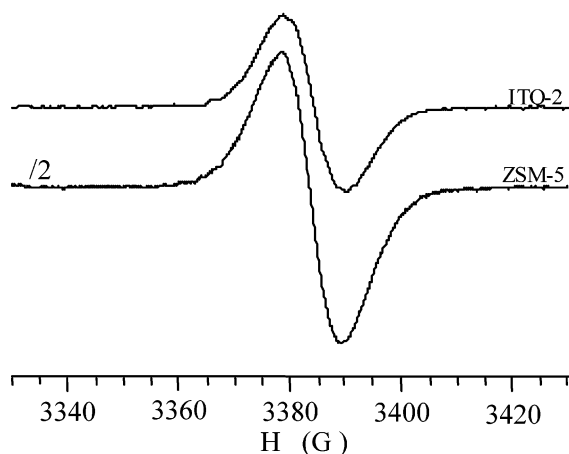


**Figure 5.** EPR spectra of DPB@ITQ-2 and DPB@ZSM-5 recorded under the same conditions three months after sample preparation. For the sake of clarity, the signal of DPB@ZSM-5 has been divided by 2.

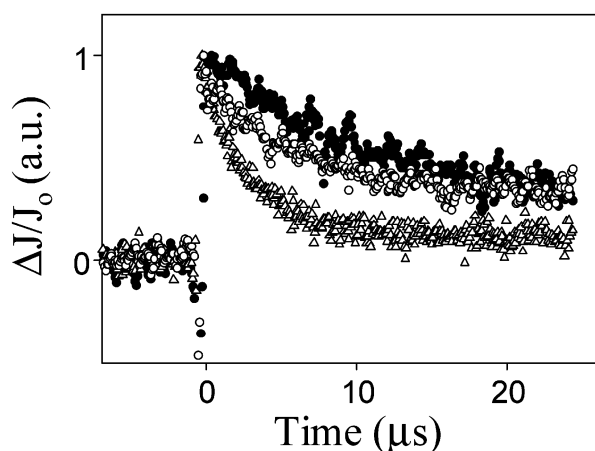


**Figure 6.** Transient decay of  $\text{TP}^+$  excited state monitored at 470 nm generated upon 355 nm laser excitation of a  $\text{N}_2$ -purged acetonitrile solution of  $\text{TP}^+\text{BF}_4^-$  ( $10^{-4}$  M): without 1-PNH (●) and after addition of 0.027 M (○) and 0.24 M (Δ) of a solution of 1-PNH in acetonitrile.

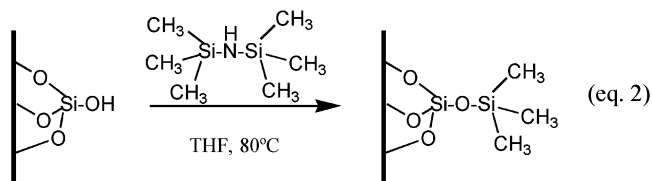
spectrum of the sample DPB@ITQ-2, laser flash photolysis generation of 1-PNH $^+$  radical cation was undertaken. The procedure followed consists of the electron transfer quenching of  $\text{TP}^+$  formed by 355 nm laser excitation by 1-PNH. Control experiments reveal that 1-PNH does not give rise to any transient using 355 nm laser at the concentrations used in the  $\text{TP}^+$  quenching. Thus, upon laser excitation  $\text{TP}^+$  is selectively formed. This  $\text{TP}^+$  triplet is quenched by 1-PNH (quenching rate constant  $1.3 \times 10^6 \text{ M}^{-1} \text{ s}^{-1}$ ) (Figure 6), and at sufficiently high concentration of 1-PNH, the transient spectrum of the  $\text{TP}^+$  triplet is replaced by that of the 1-PNH $^+$  cation radical (Figure 3 inset).

The transient spectrum of 1-PNH $^+$  cation radical obtained by photoinduced electron transfer is very similar to those previously reported in the literature for related 1-vinyl-substituted naphthalenes.<sup>31</sup> Importantly, although the resolution of the laser flash photolysis setup is lower than that of conventional UV-vis spectrophotometers, this transient spectrum is compatible with the diffuse reflectance UV-vis of DPB@ITQ-2, thus supporting the assignment of the species generated as 1-PNH $^+$ . Although it is a well-known fact, it is remarkable that 1-PNH $^+$  lifetime in solution is on the order of  $\mu\text{s}$  while inside the cyclodextrin-like cups of ITQ-2 it lives for months!

A point of the highest importance in the present report is how to justify the different behavior of ITQ-2 (generation of

1-PNH $^+$ ) compared to conventional ZSM-5 and mordenite (generation of DPB $^+$ ). In fact, our observation of 1-PNH $^+$  radical cation generation constitutes one of the clearest examples of a topologically controlled transformation due to the differences in the geometry of the zeolites. It is worth mentioning that ITQ-2 shares with classical zeolites the ability to generate a persistent population of organic radical cations (Figure 5). The question now becomes where these organic radical cations are formed. DPB is adsorbed on the straight 10 MR channels of ZSM-5. However, in the case of ITQ-2, the 10 MR channels are sinusoidal. It is, therefore, expected that the diffusion of DPB through the 10 MR sinusoidal channel must be severely restricted.<sup>15</sup> Our hypothesis is that 1-PNH $^+$  is located at the open cups of 7-Å diameter and 8-Å depth at the upper and lower planes of the layers. If this was so, we should expect that in the case of the nonlamellar MCM-22 zeolite, which has the higher amount of 10 MR sinusoidal channels but a much lesser amount of open cups than ITQ-2 (see Scheme 2), a lower number of 1-PNH $^+$  radical cations would be generated. Indeed, while the same optical spectrum is observed for ITQ-2 and MCM-22, the intensity of the signal is much higher in the former, in agreement with our hypothesis on the formation of 1-PNH $^+$  within the open external cups and not within the sinusoidal 10 MR pores.

Given the structure of ITQ-2 layers in which silanol groups are preferentially located at the rims of the cups (see Figure 1), silylation should impede the access to these cups. Thus, if the species responsible for the UV-vis spectrum of Figure 3 would be located in the main planes of the layers or within the cups, silylation should have a profound influence on the process since the access of the cups would be thwarted. On the other hand, if incorporation of DPB would occur preferentially into the 10 MR of ITQ-2 (similar dimensions as ZSM-5 but sinusoidal) then silylation of the cups should not play any significant role in the behavior of the ITQ-2. Clearly, silylation should affect a process occurring at the external surface, but not those taking place within the interior of the pores.



The degree of silylation was followed by monitoring in the IR the peak corresponding to the silanol groups. This absorption band experiences a significant decrease (about 60% of the initial band, indicating that 7 silanols out of 12 per cup have been silylated) after treatment with hexamethyldisilazane. To confirm that the presence of trimethylsilyl groups effectively impedes the access to the cups but not to the micropores, IR spectra of pyridine and 2,6-di-*tert*-butylpyridine adsorbed on a sample of ITQ-2 before and after silylation were recorded.

The comparison indicates that while the interaction of 2,6-di-*tert*-butylpyridine (too large to enter the 10 MR micropores and proving exclusively the acid sites on the external surface)<sup>14</sup> with the acid sites disappears, the amount of pyridinium formed on ITQ-2 before and after silylation only decreases in a minor percentage. This result indicates that pyridine can probe the channels of ITQ-2 equally well before and after silylation.

The diffuse reflectance UV-vis spectrum of a sample of silylated ITQ-2 after incorporation of DPB was totally different than that shown in Figure 3 and corresponds to unaltered DPB

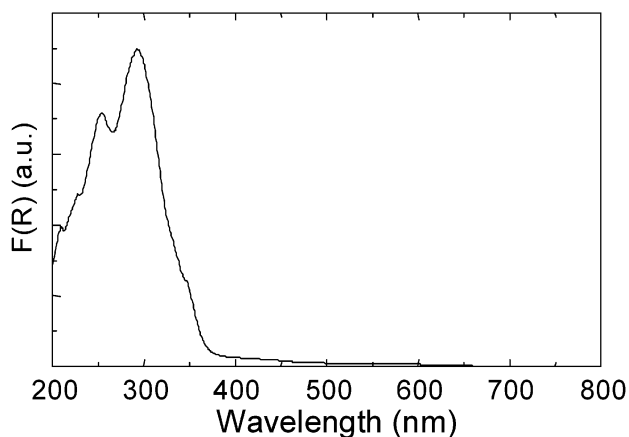


**Figure 7.** Diffuse reflectance UV-vis spectrum (plotted as the Kubelka-Munk function) of DPB@ITQ-2sil.

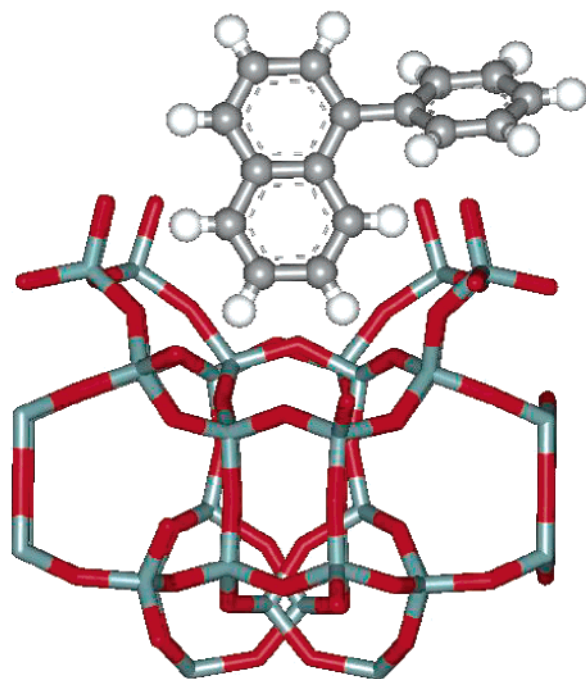


**Figure 8.** Molecular modeling showing the best docking of 1-PNH inside the cups of ITQ-2.

(Figure 7). This result firmly establishes that the ability of ITQ-2 to form the intermediate is totally suppressed by silylation. This fact together with the behavior of MCM-22 zeolite indicate that generation of 1-PNH<sup>+</sup> occurs exclusively on the external surface of the particle.

Taking into account all the evidences reported, we propose that DPBH<sup>+</sup> is initially formed in the open cups of ITQ-2 as in conventional zeolites through an acid catalysis mechanism.<sup>1</sup> But the larger conformational mobility and particularly the possibility to form cis isomers permits its cyclization toward the dihydronaphthalene skeleton.<sup>17</sup> It is this cis-trans isomerization and the subsequent intramolecular cyclization that is precluded in the channels of ZSM-5 and mordenite due to spatial restrictions. Once 1-PNH is formed, generation of its radical cation and its stabilization would occur because the shape of this molecule fits into the cups, thus undergoing the same protection as other radical cations. Figure 8 provides a molecular modeling showing the best docking of 1-PNH inside the cups of ITQ-2.

In summary, by using  $\alpha,\omega$ -diphenyl polyenes as probes we have found that novel delaminated ITQ-2 zeolites exhibit a unique behavior, shaping the radical cation that best fits within

its geometry due to a well structured external surface formed by open cups. This effect, which is clearly observed for DPB, is an example showing that the potential energy well accompanying the cups of ITQ-2 is able to generate and stabilize organic radical cations, even though the species is not deep into a channel or full pore, in a manner similar to that of the conventional medium-pore zeolite. Thus, as consequence of its special topology, the reactivity of ITQ-2 is specific and different from those of conventional zeolites.

**Acknowledgment.** Financial support by the Spanish CICYT (H.G., MAT 2000, 1768-C02-01) is gratefully acknowledged. B.F. thanks the Spanish Ministry of Education for a scholarship. We thank Dr. Carlos Gómez-García (Chemistry Department, Universitat de Valencia) for recording the EPR spectra and Dr. Germán Sastre (ITQ, Universidad Politécnica de Valencia) for molecular modeling.

## References and Notes

- (1) Liu, X.; Iu, K.-K.; Thomas, J. K.; He, H.; Klinowski, J. *J. Am. Chem. Soc.* **1994**, *116*, 11811-11818.
- (2) Ramamurthy, V.; Caspar, J. V.; Corbin, D. R. *J. Am. Chem. Soc.* **1991**, *113*, 594-600.
- (3) Ramamurthy, V. *Chimia* **1992**, *46*, 359-376.
- (4) Ramamurthy, V.; Eaton, D. F.; Caspar, J. V. *Acc. Chem. Res.* **1992**, *25*, 299-306.
- (5) Cano, M. L.; Fornés, V.; García, H.; Miranda, M. A.; Pérez-Prieto, J. J. *Chem. Soc., Chem. Commun.* **1995**, 2477-2478.
- (6) Pitchumani, K.; Joy, A.; Prevost, N.; Ramamurthy, V. *Chem. Commun.* **1997**, 127-128.
- (7) Martens, J.; Jacobs, P. A. *Adv. Funct. Mater.* **2001**, *11*, 337-338.
- (8) Davis, M. E. *Acc. Chem. Res.* **1993**, *26*, 111-115.
- (9) *Progress in Zeolite and Microporous Materials*; Chon, H.; Ihm, S.-K.; Sun Uh, Y., Eds.; Elsevier: Amsterdam, 1997; Vol. 105.
- (10) Corma, A.; Navarro, M. T.; Rey, F.; Valencia, S. *Chem. Commun.* **2001**, *16*, 1486-1487.
- (11) Corma, A. *Chem. Rev.* **1997**, *97*, 2373-2419.
- (12) Kevan, L. *J. Chem. Soc., Faraday Trans.* **1998**, *94*.
- (13) Konovalova, T. A.; Gao, Y.; Schad, R.; Kispert, L. D. *J. Phys. Chem. B* **2001**, *105*, 7459-7464.
- (14) Corma, A.; Fornés, V.; Pergher, S. B.; Maesen, T. L. M.; Buglass, J. G. *Nature* **1998**, *396*, 353-356.
- (15) Sastre, G.; Catlow, C. R. A.; Chica, A.; Corma, A. *J. Phys. Chem. B* **2000**, *104*, 416-422.
- (16) Pitchumani, K.; Joy, A.; Prevost, N.; Ramamurthy, V. *J. Chem. Soc., Chem. Commun.* **1997**, 127-128.
- (17) Pitchumani, K.; Lakshminarasimhan, P. H.; Turner, G.; Bakker, M. G.; Ramamurthy, V. *Tetrahedron Lett.* **1997**, *38*, 371-374.
- (18) Miranda, M. A.; García, H. *Chem. Rev.* **1994**, *94*, 1063.
- (19) Ramamurthy, V.; Corbin, D. R.; Kumar, C. V.; Turro, N. J. *Tetrahedron Lett.* **1990**, *31*, 47-50.
- (20) Wakamatsu, K.; Takahashi, Y.; Kibuchi, K.; Miyashi, T. *Tetrahedron Lett.* **1994**, *35*, 5681-5684.
- (21) Wakamatsu, K.; Takahashi, Y.; Kikuchi, K.; Miyashi, T. *J. Chem. Soc., Perkin Trans. 2* **1996**, *2*, 2105-2109.
- (22) Hug, S. J.; Yee, W. A.; Kligler, D. S. *Chem. Phys. Lett.* **1990**, *168*, 385-390.
- (23) Dudev, T.; Kamisuki, T.; Akamatsu, N.; Hirose, C. *J. Phys. Chem.* **1991**, *95*, 4999-5002.
- (24) Oberlé, J.; Abraham, E.; Ivanov, A.; Jonusauskas, G.; Rullière, C. *J. Phys. Chem.* **1996**, *100*, 10179-10186.
- (25) Wang, Z.; McGimpsey, W. G. *J. Phys. Chem.* **1993**, *97*, 3324-3327.
- (26) Ramamurthy, V.; Caspar, J. V.; Corbin, D. R.; Schlyer, B. D.; Maki, A. H. *J. Phys. Chem.* **1990**, *94*, 3391-3393.
- (27) Gessner, F.; Scaiano, J. C. *J. Photochem. Photobiol. A: Chem.* **1992**, *67*, 91-100.
- (28) Bae, J. Y.; Ranjit, K. T.; Luan, Z.; Krishna, R. M.; Kevan, L. *J. Phys. Chem. B* **2000**, *104*, 9661.
- (29) Krishna, R. M.; Prakash, A. M.; Kevan, L. *J. Phys. Chem. B* **2000**, *104*, 1796.
- (30) Sung-Suh, H. M.; Luan, Z.; Kevan, L. *J. Phys. Chem. B* **1997**, *101*, 10455.
- (31) Chikai, Y.; Yamamoto, Y.; Hayashi, K. *Bull. Chem. Soc. Jpn.* **1988**, *61*, 2281-2285.
- (32) Argauer, R. J.; Landolt, G. R. U. S. Patent 3,702,886, 1982.
- (33) Mohtat, N.; Cozens, F. L.; Scaiano, J. C. *J. Phys. Chem. B* **1998**, *102*, 7557-7562.